# The Colors of Proxy Noise

Mara Y. McPartland<sup>1</sup>, Thomas Münch<sup>1</sup>, Andrew M. Dolman<sup>1</sup>, Raphaël Hébert<sup>1</sup>, Thomas Laepple<sup>1,2</sup>

<sup>1</sup>Alfred-Wegener-Institut Helmholtz-Zentrum für Polar- und Meeresforschung, Research Unit Potsdam, Potsdam, Germany

<sup>2</sup>MARUM—Center for Marine Environmental Sciences, University of Bremen, Bremen, Germany *Correspondence to*: Mara Y. McPartland (mara.mcpartland@awi.de)

### Abstract.

5

The complex biological and physical processes that preserve paleoclimate information over centuries or 10 longer introduce variations in proxy time series that are unrelated to the true climate. These nonclimatic variations act on different timescales and are often referred to as "noise" of a specific color. based on similarities between the time series' power spectrum and the electromagnetic spectrum of light. For example, "white noise" equally affects all timescales, where "red noise" dominates only on long timescales, similar to longwave red light. Noise spectra in proxy records have far-reaching 15 implications in paleoclimate research, but noise characteristics are often assumed based on first principles rather than estimated directly, risking either inflating or underestimating error at particular frequencies. Here, we provide concrete definitions of the various types of timescales-dependent errors that are present in proxy data, and review the literature on methods for quantifying noise terms. We then synthesize the results of several published studies that use a common empirical approach for estimating the noise spectrum in ice core, coral, and tree-ring data. We posit that the colors of proxy noise are 20 archive-specific, with white noise dominating in depositional archives such as ice cores and marine sediment cores, while red noise is more common in biological archives such as tree rings and corals. Our synthesis supports assigning specific colored noise terms in proxy system models, data assimilations and other experiments.

### 25 1 Introduction

30

Paleoclimate proxy records archive past climate information via biophysical or depositional pathways and preserve it in rings, layers or strata. The processes that create these records integrate non-climatic variability alongside the climate signal either during the archiving process, or afterwards as the physical record is modified over time (Cook 1987; Evans *et al.*, 2013). Recovering paleoclimate information from these archives requires sophisticated data processing and modeling techniques intended to extract climate-related variance from noisy time series (von Storch *et al.*, 2004; Cook & Kairiukstis 1990; Hughes & Ammann 2009; Dee *et al.*, 2016). Recognizing that these methods may be imperfect, the challenge lies in rigorously quantifying and minimizing the impact of non-climatic variations on the signal of past climate changes.

Climate Signal 40 Archive/Sensor **Noise** age-growth trends life history effects layer deformation drifting & redistribution 50 **Smoothing** biological memory isotopic diffusion bioturbation **Observation &** measurement error **Data Processing** Detrending Bioturbation deconvolution Age-depth modeling Pre-whitening Diffusion correction Calibration 70 **Reconstructed Time Series** 

Figure 1: Conceptual diagram showing integration of different types of timescale-dependent proxy errors alongside climate signals via stochastic noise and subtractive smoothing.

deposition or uncertainties in dating, or a combination of these effects (Fig. 1). We regard a process that adds variance on top of an existing climate signal as a "noise process", whereas the loss of variance through smoothing also constitutes error (i.e., any difference between the true and reconstructed climate at a given timescale), but not technically noise. Smoothing processes are typically deterministic to some extent. For example, two co-located ice-core records with similar physical properties are both affected by same isotopic diffusion and their correlation at a certain time-scale will not be affected if there is no additional noise (Whilans & Grootes 1985). It is further possible to correct individual records for deterministic errors if the process is well-understood (Shiffelbein 1985: Meko 1981; Dolman et al., 2021a; Shaw et al., 2023). By contrast, noise is typically independent, generating differences between nearby records as well as to the true climate signal. Observation and measurement errors are best represented by stochastic, uncorrelated noise unless they represent systematic bias, for example due to a change in the measurement apparatus. Because these types of noise are typically independent, averaging, or "stacking" individual records reduces noise while retaining the climate signal.

Both noise and smoothing processes incorporate unique timescale-dependent uncertainties alongside climate signals. For example, trees integrate multi-decadal agegrowth trends alongside climate variations, such that treering time series are typically 'detrended' before they are used in reconstructions (Fritts 1976; Cook & Kairiukstis 1990; Speer 2010). Incomplete removal of age-growth trends results in long-term biases in tree-ring data, even if interannual correlations with climate data remain reasonably strong (Melvin & Briffa 2008; Melvin & Briffa 2014 a,b). By contrast, physical smoothing processes such as isotopic diffusion or bioturbation in sediments act on fast timescales by removing climate information from within deposited layers (Johnson et al., 2000; Whillans & Grootes 1985; Hutson 1980; Peng & Broeker 1984). Smoothing

dampens the climate signal at annual to centennial timescales, becoming less influential on longer timescales such that millennial-scale shifts in climate are retained (Schiffelbein & Hills 1984; Laepple & Huybers 2013; Münch & Laepple 2018; Bothe et al., 2019).

80

85

90

These timescale-dependent variations can be analyzed in the spectral domain and referred to using colors by loose analogy to the frequency spectrum of light (Fig 2). Time series with relatively more low- than high-frequency variability are considered to be 'red', by analogy to long-wave red light, whereas a 'white' time series implies that power spectral density is distributed evenly across the frequency space.

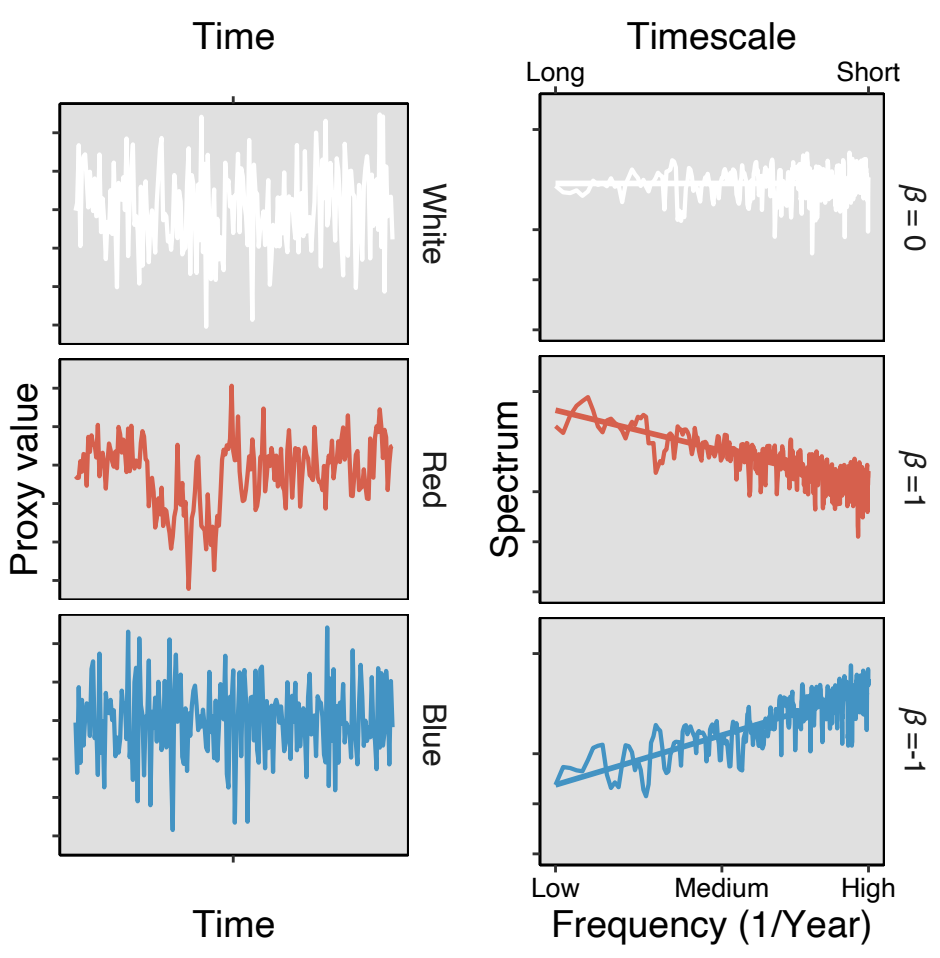


Figure 2: Spectral noise models with correlation structures referred to by analogy to colored light. Left panels show a simulated time series with the noise spectra shown in the right panels. Top: white noise with no correlation with timescale ( $\beta = 0$ ). Middle: red noise (sometimes referred to as pink noise) with a positive relationship to timescale ( $\beta = 1$ ). Bottom: blue noise with a negative relationship to timescale ( $\beta = -1$ ). Note that  $\beta$  values for noise spectra are calculated as the slope of a linear model on a log-log plot, and expressed as  $\beta$  = slope\*-1, following the convention where  $\beta$  describes the relationship between power and timescale.

Low-frequency temperature variability is generally understood to exhibit increasing power with timescale, meaning that noise-free temperature proxy spectra would theoretically display a red spectrum

# Power-law scaling in frequency space

- The spectral exponent β summarizes the relative contribution of high- and low-frequencies to the total variance.
- The power spectral density S(f) is assumed to approximately follow a power-law with frequency f such that S(f) ~f<sup>β</sup>
- β is typically expressed as the negative slope of a linear regression on a log-log plot of the power spectrum.

Box 1: Summarizing the timescale-dependency of proxy noise using spectral power-laws.

25

30

(Pelletier 1998; Huybers & Curry, 2006; Zhu et al., 2019). Noise, because it originates from a variety of sources may display different correlation structures. The integration of noise and climate signals may either further 'redden' or 'whiten' the spectrum by modifying the correlation structure of the raw time series. The relationship between power spectral density S(f) and frequency f is often summarized using a power-law scaling exponent  $\beta$  such that  $S(f) \sim f^{\beta}$  (Box 1) (Vautard & Ghil 1989, Fraedrich & Blender 2003; Hébert et al., 2021). The exponent  $\beta$  represents the relationship between frequency (or time period) and power spectral density, which appears as a linear relationship plotted on a log-log scale. By convention, the exponent is defined as the

negative of the relationship with frequency such that a positive exponent actually represents increasing variance with timescale. Red noise processes are represented with a positive slope value (β>0); the term 'pink noise' is sometimes used specifically for β=1 (Zhu et al., 2023). Red noise is a common noise model that implies autocorrelated errors that affect low-frequencies at a greater magnitude. (Mann et al., 2007; von Stoch et al., 2009; Smerdon 2012). By contrast, a 'white' noise process implies errors uncorrelated in time such that the variance is distributed evenly across the frequency space (β=0), similar to the spectrum of white light. White noise is the simplest and most commonly-applied noise model in paleoclimate research (Fisher et al., 1985, Amman & Whal 2007; von Storch et al., 2004; Mann et al., 2005, Lee et al., 2008; Smerdon et al., 2010; 2012). Finally, blue noise refers to processes with relatively higher variability at high frequencies (β<0). Blue noise is characterized by an anti-correlated structure, implying rapidly vanishing effects with increasing timescale (Mann & Rutherford 2002; Mann et al., 2007).</li>

Our understanding of proxy noise characteristics has evolved out of the need to reconcile diverging results in records that should, in principle, contain the same climate signal. For certain processes, such as the effects of measurement error, aliasing due to under-sampling, or depositional noise from roughness at the snow surface, the noise power spectrum can be derived from first principles and expressed in closed-form solutions (Fisher *et al.*, 1985; Schiffelbein, 1985; Kunz *et al.*, 2020; Dolman *et al.*, 2021b). In cases where the physical and biological processes affecting proxies are well-understood, a more flexible approach is to use proxy system models (PSMs) (Jones *et al.*, 2009; Vaganov *et al.*, 2011; Evans *et al.*, 2013; Tolwinski-Ward *et al.*, 2011; Dee *et al.*, 2016; Dee *et al.*, 2017; Dolman and Laepple, 2018). In this case, climate data sets of temperature and precipitation from instrumental data, climate models or stochastic simulations are used as input to the PSM, and synthetic proxy time series are simulated. The spectrum of the noise can then be estimated through comparison to the climate time series (Dee *et al.*, 2017). By omitting processes that are not well-understood, PSMs

35 may underestimate the noise level. For example, stratigraphic noise in ice-core-based proxies can account for more than half of the isotope signal (Hirsch *et al.*, 2023) but stratigraphic processes are not represented in current isotope PSMs (Dee *et al.*, 2015). To account for "known unknowns" recent studies have added estimates of noise with specific spectral properties to mimic these extraneous sources of variability in PSM output, using models or reanalysis data as external validation. (Dee *et al.*, 40 2018; Evans *et al.*, 2014; Zhu *et al.*, 2023; Bothe *et al.*, 2019).

Alternatively, empirical proxy noise spectra can be derived by relying solely on proxies by exploiting the spatial correlation of climate signals in nearby records, building on the assumption that non-climatic noise is independent between records. This approach has the advantage of being able to exploit the full length of paleoclimate time series without relying on climate models or short instrumental time series, and without the assumption that physical processes themselves are well-understood. One limitation is that this method relies on the availability of replicated or nearby records that have low time-uncertainty, such as corals, tree rings, and banded ice cores or laminated sediments. If empirical noise estimates are consistent with those derived from mechanistic models this both validates the processes represented in PSMs creates a strong basis for using the resulting noise spectra in a variety of research applications.

In this study, we synthesize noise estimates derived directly from multiple proxy types and interpret their spectral characteristics in the context of known biological and physical processes. This provides a basis for evaluating signal fidelity and for refining assumptions commonly made in proxy system models and other experiments. We present noise estimates published in three studies where noise terms were derived using a simple empirical approach that partitions shared signal from independent variance on all timescales (Münch & Laepple 2018), which we describe in the extended data section (Appendix A). We show results for published ice cores from Münch & Laepple 2018, tree rings (McPartland *et al.*, 2024), and corals (Dolman *et al.*, in revision). By presenting these findings alongside evidence from first principles and existing literature we aim to deepen a collective understanding of the behavior of proxy noise.

The tree-ring and coral data were sourced from global databases compiled by the Past Global Changes (PAGES) initiative (PAGES Consortium 2017; Walter *et al.*, 2023), and the ice-core data represent two large clusters of cores from Antarctica and Greenland (Graf *et al.*, 2002; Weißbach *et al.*, 2016; Hörhold *et al.*, 2023) (Appendix B). Full details on each result are provided in the aforementioned studies. We focus our discussion on the noise spectra and resulting signal-to-noise ratio. Evaluating the climate signal spectra would ideally involve comparison with data and models, which are beyond the scope of this paper. In the extended data section, we reproduce the signal spectra and sample density at each frequency to provide all information involved in the noise spectra calculations and their uncertainty estimates (Appendix C).

# 2 The colors of proxy noise across paleo archives

45

50

55

60

65

70

Our review of published noise estimates demonstrates that tree rings and corals exhibit clear red noise spectra with positive scaling exponent  $\beta$  values of 0.8 and 0.5 respectively (Fig 3; a, b) such that the

power of the noise increases with timescale (McPartland *et al.* (2024), Dolman *et al.* (in revision). As the noise increases more than the climate signal, this leads to a decline of the signal-to-noise ratio (SNR) (Fig 3; d, e). Tree-ring and coral records result from the *growth* or *accretion* of layers by an individual organism over time such that life history or changes in the biological archiving system may affect proxy formation. Evidence suggests that proxy records composed of repeated measurements made on single long-lived organisms through time are susceptible to ontogenetic effects, the legacies of past disturbances, or slow changes in the behaviour of the sensor.

80 In dendroclimatology, the pitfalls associated with tree ontogeny have been well-documented (Fritts 1976; Cook et al. 1995; Esper & Frank 2009). Cambial age impacts both tree-ring width and density such that detrending to remove juvenile age trends is a near universal practice (Cook & Kairiukstis 1990). Even after detrending, residual age effects could partially explain the persistent low-frequency bias observed in tree-ring records (Franke et al., 2013, Ault et al., 2013). Detrending itself can also 85 introduce biases at medium-frequencies, particularly when fitting raw time series with negative exponential curves, regional curves or rigid spline functions (Cook & Peters 1997; Melvin & Briffa 2008; Melvin & Briffa 2014 a;b, Esper 2003, Briffa & Melvin 2011). Techniques such as "signal-free" detrending have aimed at boosting low-frequency variability while minimizing bias (Melvin & Briffa 2008), but despite retaining more low-frequency variance, tests of this method indicated only minor 90 improvements in signal strength and signal-free chronologies retained their red-noise spectra (McPartland et al. 2020; McPartland et al. 2024). By extension, red noise is likely a feature of bivalve and sclerosponge chronologies, which contain similar age-growth trends to those found in trees and are detrended using the methods originally developed in dendrochronology (Jones 1983; Rypel et al. 2008; Hollyman et al., 2018; McCulloch et al., 2024). Tree rings are also smoothed on fast timescales as a result of the carryover, or 'memory', of prior years' growth. Biological memory adds temporal 95 autocorrelation to tree ring time series which has the effect of steepening the slope of the noise spectra by reducing high frequency power spectral density (Zhang et al. 2015; Lucke et al. 2019; McPartland et al. 2024). 'Pre-whitening' chronologies by adjusting their temporal autocorrelation structure to match the climate target improves the interannual correlation between data and proxy (Meko 1981), but by virtue of removing additional variability at high-frequencies, decreases the ratio of high to low power 00 spectral density that defines the noise slope term  $\beta$ .

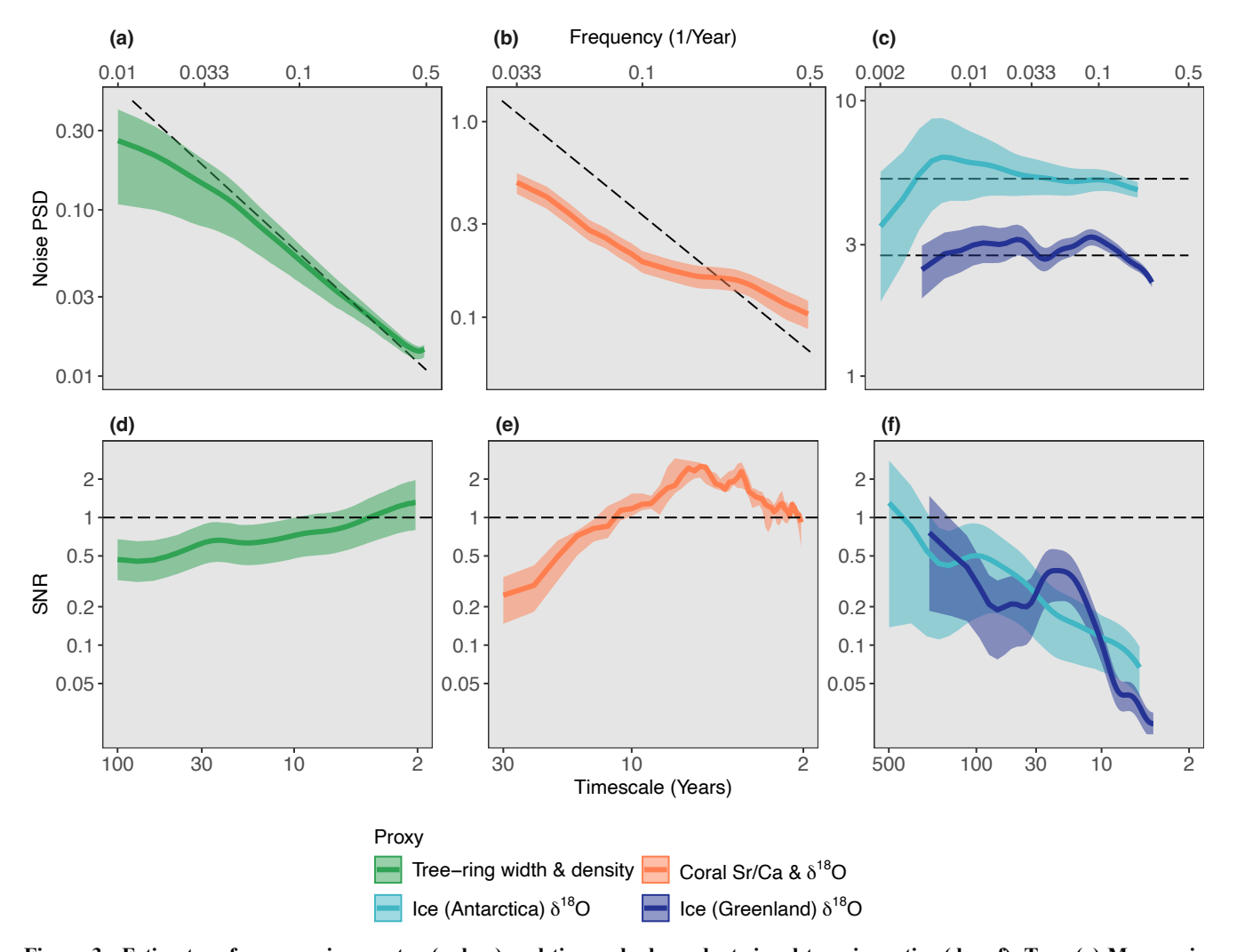


Figure 3: Estimates of proxy noise spectra (a, b, c) and timescale-dependent signal-to-noise ratios (d, e, f). Top: (a) Mean noise spectra for tree-ring width and density records from northern hemisphere tree-ring records, (b) Mean noise spectra for tropical coral  $\delta$  O and strontium/calcium (Sr/Ca) ratios, (c) Noise spectra for ice core  $\delta$  O from Dronning Maud Land (light blue) in Antarctica and the North Greenland Traverse (dark blue). Dashed lines represent an idealized spectral power-law with a slope  $\beta$  = 1 for proxies containing predominantly red noise (i.e. tree rings and corals), and with  $\beta$  = 0 for proxies (i.e. ice cores) containing predominantly white noise. Bottom: Timescale-dependent signal-to-noise ratios (SNR) for (d) tree rings, (e) corals, and (f) ice cores. Dashed lines represent an SNR of 1. Confidence intervals on all spectra represent the 10th and 90th percentiles from a parametric bootstrapping estimation method. Detailed methods for estimating proxy noise and SNR values can be found in McPartland *et al.*, (2024) (tree rings), Münch *et al.*, (2018) (ice cores) and Dolman *et al.*, (under revision) (corals).

Coral aragonite records might similarly be affected by changes in the biology of individual or descendent polyps over time resulting in a slow drift in the temperature response of the proxy which would appear as low-frequency variability. Such changes could be growth-rate related due to reaction-kinetic effects (Goodkin *et al.*, 2005; Hayashi *et al.*, 2013; Maier *et al.*, 2004; Saenger *et al.*, 2008;

Suzuki *et al.*, 2005), result from changes in the calcification process (Lough 2004), or persistent baseline shifts in trace element ratios following thermal stress events (D'Olivo & McCulloch 2017; D'Olivo *et al.*, 2019) perhaps mediated by changes in the composition of photosynthetic symbionts (Berkelmans & van Oppen, 2006; Cohen, 2002; Little *et al.*, 2004).

20

25

30

35

40

45

50

55

The stacks of ice cores from both Greenland and Antarctica that we analyzed show a high white noise level where  $\beta$  is approximately equal to zero (Fig 3 e, f) (Münch & Laepple 2018). As the climate variations become more pronounced on longer timescales, this leads to an increasing signal-to-noise ratio with time. We argue that proxies that are primarily the result of deposition, rather than growth or accretion primarily contain white noise stemming from stratigraphic processes. Precipitation intermittency and post-depositional redistribution in ice cores result in adjacent measurements that represent water from different precipitation events (Laepple et al., 2018; Casado et al., 2020; Zuhr et al., 2023). By extension, in marine sediments where foraminifera or diatoms are deposited from the water column, each sample represents a new set of individuals such that biological effects are uncorrelated between measurements. From process-based experiments, it has been demonstrated that noise in sediment records is also predominantly white with the signal level increasing as more individuals are measured (Kunz et al., 2020, Dolman et al., 2021). In both ice and sediment core records of near-surface temperature, seasonal depositional cycles are much stronger than any interannual or even millennial climate change and the sparse subsampling of the seasonal signal leads to aliasing of independent noise within the signal of annual variation (Kunz et al., 2020). Precipitation intermittency and depositional redistribution break up the signal of the large seasonal cycle that would appear as a large spike in the spectrum at annual timescales if the signal were recorded without disruption. Instead, the spike is redistributed as white noise across all frequencies (Casado et al., 2020; Münch et al. 2021).

We identified fewer examples of blue noise processes in the paleoclimate literature. Because its effects diminish quickly with time, blue noise does not introduce error past fast timescales. An example of a true blue noise process is the infilling of troughs on ice sheets as wind redistributes snow causing blue noise in annual layer thickness records from ice cores (Fisher *et al.*, 1985). Blue noise models have occasionally been tested alongside red and white noise to account for a variety of potential types of error affecting high-frequencies, and to improve the fit between synthetic proxy records and climate model data (Mann *et al.*, 2007; Mann & Rutherford 2002).

Like blue noise, smoothing processes predominantly affect high frequencies and becomes less significant with timescale. Biological memory in trees, diffusion in ice cores, and bioturbation in sediments are all examples of smoothing processes that lead to correlated errors between the climate and the proxy signal which theoretically can be accounted for using deterministic modeling (Matalas *et al.*, 1962; Berger *et al.*, 1977; Meko 1981; Ruddiman *et al.*, 1980; Whillans and Grootes, 1985). Given such a model, the smoothing effect can be reversed, as we applied in this example to ice core data to reverse the effects of diffusion (Shaw *et al.* 2024) (see Appendix A). If, as in the case of diffusion, the smoothing process affects the signal and the noise equally, the SNR is unbiased at all timescales regardless of whether or not a correction for the smoothing effect is applied. However, when noise is introduced after smoothing (e.g. measurement noise), the attenuated climate signal on the high-

frequency side will be masked by a relatively stronger noise level, biasing the SNR spectrum downwards toward high frequencies. In any case, knowledge about and accounting for smoothing processes in paleoclimate time series is critical for evaluating the short-term effects of climate forcing events such as volcanic eruptions (Esper *et al.*, 2015; Zhang *et al.*, 2015; Lücke *et al.*, 2015), but is potentially less critical for reconstructing low-frequency variations in climate.

# 3 Time uncertainty and noise color

- Dating for all three proxy types discussed here is primarily achieved by some kind of band dating, or by counting annual cycles in geochemical tracers. If bands or cycles are missed, or double counted, this introduces time-uncertainty and an additional source of error in the reconstructed climate time series (Comboul *et al.* 2014). Time uncertainty has little effect on the shape of individual power spectra when the spectra are broadband, as is typical for climate time series (Rhines & Huybers, 2011). However, it reduces coherence between records, diminishing high-frequency power in stacked spectra and biasing SNR estimates downward at shorter timescales (Münch & Laepple, 2018; Fig. D1). The effect of time-uncertainty acts as a linear transfer function on the stacked spectra and can be estimated and corrected for if the time uncertainty is known, although this was not applied here (Appendix D). For the ice-core records analysed here, the time-uncertainty is due to potential variations in the accumulation rate between volcanic tie-points and is negligible for frequencies below 1/10 years (Münch & Laepple 2018, their Fig. B1).
- For the sub-annual resolution coral records used here, age models mostly come from counting annual cycles in the geochemical tracers. However, for most coral records there are no independently dated tie-points and so it is not possible to directly estimate counting error rates and correct for time-uncertainty. Simulations with potential error rates derived from corals show that the slope of the SNR is biased in the opposite direction to the one we estimate (Fig. D1) and that even for very large error rates of 1 in 10 years' time-uncertainty cannot account for the low SNR at decadal timescales. Time uncertainty is arguably less of an issue for tree-ring records as they are considered to be precisely dated and dendrochronologists routinely employ statistical cross-dating techniques to identify and eliminate dating errors (Holmes et al 1986). Through this process locally absent rings are identified during cross-dating and assigned a no-data value to avoid affecting the final chronology. The strength of the tree-ring SNR on sub-decadal timescales is indicative of this dating precision.
- For proxy archives that are not annually resolved such as reconstructions from non-varved terrestrial and marine sediment cores, the irregular spacing of samples in time and larger dating uncertainties makes stacking unsuitable for this type of noise estimation, representing a limitation of this approach. Alternative methods, such as estimating the SNR as a function of time uncertainty (Reschke *et al.*, 2018), or applying tuning methods that align proxy records by maximizing covariance and assess significance against surrogate data (Haam & Huybers, 2010), may still allow for empirical SNR estimation in these cases.

# 4 Implications of colored noise for climate reconstruction

00

05

20

25

30

The spectrum of temperature on local to global scales is generally accepted to be red (Huybers & Curry 2006; Cheung *et al.*, 2017; Hasselmann *et al.*, 1976). For proxies with predominantly white-noise spectra such as ice cores and sediments, this implies that the power spectral density of the climate signal relative to the noise, the SNR increases with timescale. This explains why ice cores are faithful recorders of millennial climate variability (e.g. EPICA, 2006), while they fail in many regions to reconstruct interannual to decadal changes (Stenni *et al.*, 2017). By contrast, in proxies that contain red noise, the SNR will rise more slowly or even decline with timescale if the power of the noise rises more steeply than the signal, as we demonstrate in tree rings and corals. These proxies are better recorders of fast time-scale variability where the ratio of signal to noise is highest. For example, corals can deliver unique information on tropical climate dynamics such as the El Niño Southern Oscillation (ENSO) (Fig. 3), but have challenges reconstructing multidecadal trends (Scott *et al.*, 2010).

The color of the noise thus influences the timescales at which a robust climate signal can be reconstructed, because it introduces a frequency-dependence to the SNR. Information about proxy noise can be used to guide future study design (e.g. what proxies can be used to answer a climatic hypothesis) and to optimize the sampling and measuring design (e.g. how many cores are needed; what is the optimal sampling resolution to minimize noise). It can also be used to estimate time scale-dependent uncertainty in climate reconstructions. For individual proxy time series where the signal increases more strongly with timescale than the noise, when the signal spectrum is "redder" than the noise, binning to a coarser timestep or by applying stronger smoothing reduces the noise. This improves the SNR, albeit at the cost of losing information at shorter timescales. The extent to which uncertainty is reduced by binning or smoothing depends on the relative spectral slopes of both the signal and noise.

Knowing the color and level of proxy noise is valuable for a variety of research contexts in paleoclimatology. For example, accurate noise models are important for pseudo-proxy experiments (PPEs) in which climate model output is degraded into pseudo-proxy time series to test the skill of reconstruction methods and evaluate models (Jones *et al.* 2009; Smerdon *et al.* 2012). Often PPEs rely on sensitivity tests using different noise levels or spectral colors (Riedywl *et al.* 2009; Smerdon *et al.*, 2010; Mann and Rutherford, 2002; Gomez-Navaro *et al.* 2017). Red noise is often tested alongside white or sometimes blue noise, but typically using a first-order autoregressive (AR(1)) process with a fixed spectral slope ( $\beta = 2$ ) (Mann *et al.* 2007; Riedywl *et al.* 2009). However, this can lead to underestimation of the actual noise, especially at low frequencies where the spectrum of an AR(1) process levels out. More recent PPEs have integrated full PSM complexity with realistic noise estimates (Boothe *et al.* 2019; Zhu *et al.* 2023). Finally, accurate noise estimation is important in data assimilations and field reconstructions to bring reconstructed time series into better alignment with calibration datasets, and to propagate uncertainty in estimates of past climate variability (Goose *et al.* 2010; King *et al.* 2021).

### 35 Conclusion

40

45

50

55

Building on prior insights from proxy system modeling, and with reference to a first-principles based understanding of proxy formation, we present here an overview of how colored noise is represented in different types of paleoclimate archives. Incorporating empirical, proxy-specific noise models as presented here into a range of paleoclimate research activities will help to move away from the assumption that noise is white or follows a first-order autoregressive process, which can lead to misinterpreting noise as signal and propagating biases into results. These noise models, or models derived using similar stacking and variance-partitioning methods, can be used account for the range of unique biological and physical processes affecting proxies in pseudo proxy experiments, data assimilation frameworks, and reconstructions efforts to improve the representation of patterns of past climate variability.

# **Appendix**

# **Appendix A: Estimating the spectrum of noise**

We apply the method of Münch *et al.*, (2018) of combining clustered proxy records into regional stacks and analyzing their variance in the frequency domain. This builds on the assumption that the proxy signal is a function of four main components: the climate signal, additive noise that arises during the proxy creation and archiving stages, measurement noise, and any smoothing processes that act during archiving but not on the measurement noise; i.e.

$$\mathcal{P} = f(\mathcal{C}, \mathcal{N}, \Sigma; \mathcal{G}) = \mathcal{G}(\mathcal{C} + \mathcal{N}) + \Sigma$$

where P, C, N, and  $\Sigma$  stand for the power spectral densities of the proxy signal, the climate signal, the proxy noise, and the measurement noise, respectively, and where G is a transfer function that describes a specific smoothing process such as biological memory, diffusion, or bioturbation.

Given a regional cluster of *n* proxy records with a similar climate between sites, the mean power spectrum, *M*, averaged across all individual records' spectra, will yield a precise estimate of the proxy spectrum *P*. By contrast, the power spectrum, *S*, of the stacked record from averaging all records in the time domain, will also contain the full climate signal, but with the noise proportions reduced by a factor of *n*. By combining both quantities one can derive expressions for the climate and noise spectra (Münch and Laepple, 2018),

$$\mathcal{C} = \frac{n}{n-1} \mathcal{G}^{-1} \left( \mathcal{S} - \mathcal{M}/n \right); \quad \mathcal{N} = \frac{n}{n-1} \mathcal{G}^{-1} \left( \mathcal{M} - \mathcal{S} - \frac{n-1}{n} \Sigma \right)$$

with the ratio of *C:N* yielding the frequency-resolved signal-to-noise ratio (SNR). A common smoothing process equally biases the signal and the noise spectrum, if not corrected for by means of the inverse transfer function *G*<sup>-1</sup>, and hence its effect cancels out in the SNR spectrum. We note that time uncertainty between individual proxy records can be another source of smoothing in the stacked record, but it is less straightforward to include into our methodology (Münch and Laepple, 2018) and is neglected here.

# **Appendix B: Data**

# **B.1 Tree Rings**

For the tree-ring data we analyzed the tree-ring records contained within the Past Global Changes 2k (PAGES2k) database, a large database compiled to reconstruct global temperature variations during the last two millennia. This network of 647 unique paleoclimate records from around the globe includes 450 tree-ring time series, of which we used 421 records of tree-ring width and density located across the Northern hemisphere (PAGES 2013, 2017; Neukom *et al.*, 2019). Spatial clusters were defined using 250-kilometer radii, such that no two sites were more than 500 kilometers apart. Tree-ring width and density records were clustered separately so that the proxies weren't mixed within clusters. This resulted in 253 clusters containing a minimum of 3, and a maximum of 30 sites per cluster. The average length of the overlapping period was around 450 years. The results of all clusters of both proxy types were averaged at the end to derive the signal, noise and SNR. Uncertainty was calculated using a parametric bootstrapping approach. (McPartland *et al.*, 2024).

#### **90 B.2** Corals

95

05

We used the coral records contained within the PAGES Coral Hydro 2k database to obtain coral SNR estimates (Walter *et al.*, 2023). The Coral Hydro2k database contains 54 oxygen ( $\delta^{18}$ O) and strontium calcium (Sr/Ca) records from the global tropics. The database was compiled to reconstruct sea surface temperature and ocean hydroclimate variability for the past two centuries. Due to fewer records, 1000 km spatial clusters were used, resulting in 64 clusters.  $\delta^{18}$ O and Sr/Ca records were clustered separately and the results were averaged. More information on the coral data curation is contained in Dolman *et al.*, *under revision*.

### **B.3 Ice Cores**

As an example for ice-core derived temperature proxies, we use stable isotope records from the Dronning Maud Land region in Antarctica ("DML data" in the following; Graf *et al.*, 2002) and from central-north Greenland ("NGT data" in the following; Weißbach *et al.*, 2016, Hörhold *et al.*, 2023).

The DML data consist of 15 records, 12 of which cover the time period from 1800 to 1998 CE and 3 records cover 1000–1998 CE. We combine both datasets by using the individual spectral results (Münch and Laepple, 2018) of the shorter records on timescales below decadal and of the longer records on the

supra-decadal timescales. We apply the diffusion correction as in Münch and Laepple (2018) but do not use their time-uncertainty correction.

The NGT data comprise 14 cores covering the time span from 1505 to 1979 CE, including original records from the North Greenland Traverse published in Weißbach et al (2016) as well as the extended NGT records from exploiting new drillings as presented in Hörhold *et al.*, (2023). The corresponding NGT spectra shown in Hörhold *et al.*, (2023) were not diffusion-corrected; here, to be able to compare the NGT spectra to those from the DML data, we apply a diffusion correction to the NGT spectra following the method given in Münch and Laepple (2018) with diffusion length estimates calculated as described in Hörhold *et al.*, (2023). Note that the SNR spectrum shown in Hörhold *et al.*, (2023) used the ratio of the integrated signal and noise spectra, which is related to the correlation with the climate signal (Münch and Laepple, 2018), whereas here we show the direct ratio of the spectra.

# Appendix C: Signal, noise and signal-to-noise ratio estimation

Full results for the uncorrected signal, noise and SNR estimates for tree rings, corals and ice-core data (Fig. A1 a,b,c,d). Spectra in Fig. 3 represent truncated versions which have been cut off where sample density in corals and tree rings drop off (shaded regions), as seen in the spectral density plots (Fig A1 bottom panels). In both corals and tree rings, the SNR rises again due to the reduction in replication and dominance by single or a small number of records with higher SNR than average (Fig A1, a,b) (see McPartland *et al.* 2024; Fig 2, e,f). Confidence intervals on all spectra represent the 10th and 90th percentiles from a parametric bootstrapping estimation method. In addition to the truncation due to low sample size, the lowest two spectral estimates on all spectra are removed during SNR calculation and confidence interval estimation a the multitaper approach introduces a small bias at the lowest frequencies (Percival & Walden, 1993).

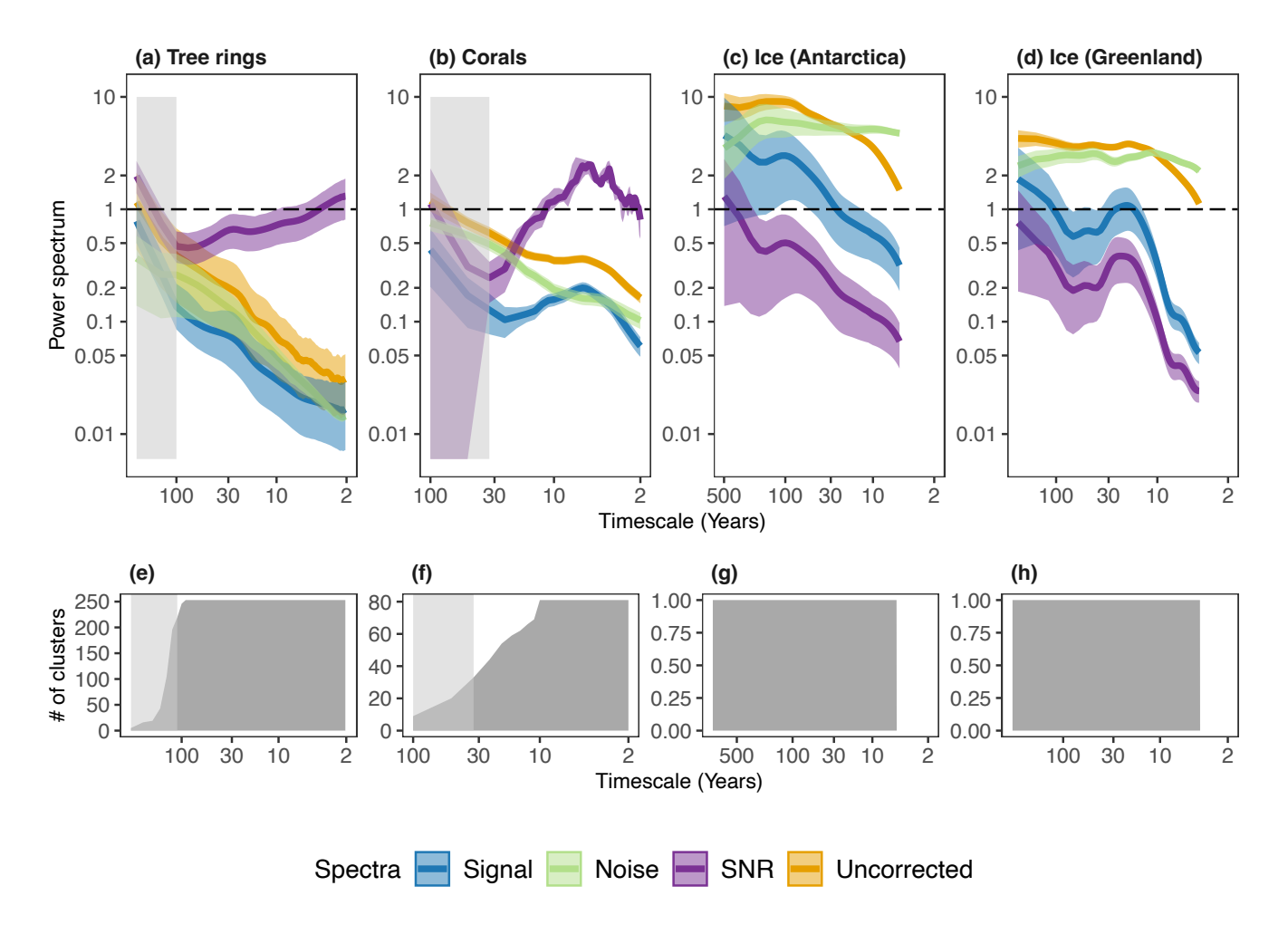
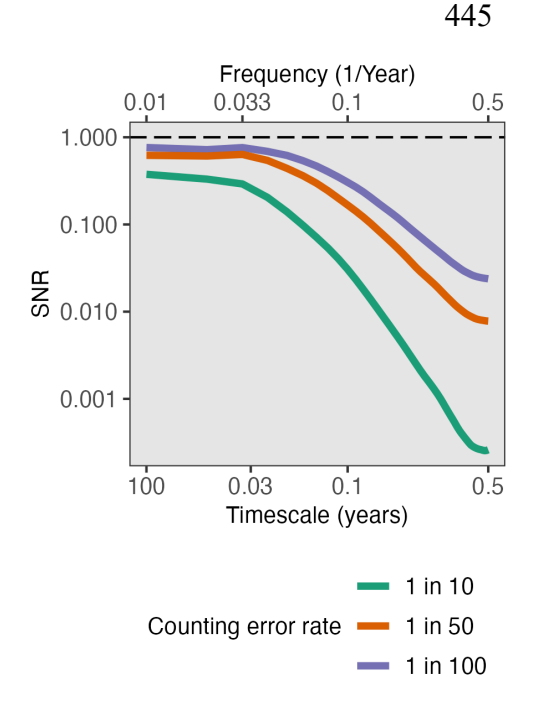


Figure C1: Timescale-dependent signal, noise and SNR estimates with sample density plots for tree-rings (a,e), corals (b,f), and ice-core δ<sup>18</sup>O data from Dronning Maud Land in Antarctica (c,g) and the North Greenland Traverse (d,h). Top graphs show signal (blue), noise (green) and SNR (purple) curves, with the uncorrected "proxy" spectra (yellow). Confidence intervals on all spectra represent the 10th and 90th percentiles from a parametric bootstrapping estimation method. The light grey shading indicates the cut-off point for spectral estimates presented in Fig. 3 when sample density decreases and the results become more uncertain. Detailed methods for estimating proxy noise and SNR values can be found in McPartland et al., (2024) (tree rings), Münch et al., (2018) (ice cores) and Dolman et al., (under revision) (corals).

# Appendix D: Simulated effects of time uncertainty on timescale-dependent signal-to-noise ratios

To illustrate the potential effects of time uncertainty on estimates of signal-to-noise ratio we used the approach of Comboul *et al.* (2014) as implemented by Münch and Laepple (2018). Münch and Laepple (2018) show that relative time-uncertainty between records in a stack acts as a linear transfer function, reducing power in the stack at high frequencies. The precise shape of the transfer function depends on the counting error rate, and on the lengths of the time series, as longer time series allow larger relative



errors to accumulate. It does not depend on the power spectrum of the initial "true" signal. Here we show the effect on SNR for 100-year time series with band counting error rates of 1 in 10, 50 and 100 years, with equal probability of missing or double counting a band. The effect on estimated SNR is shown relative to a hypothetical true SNR of 1.

 $\tau \upsilon \iota$ 

Figure D1: The influence of timeuncertainty on SNR estimated by the stacking method. Here time uncertainty is simulated for a set of 100-year records with band counting error rates of 1 in 10, 50 and 100, and a true SNR of 10 at all frequencies. The simulation was carried out following Münch and Laepple (2018) which implements the counting error model of Comboul et al. (2014).

# **Data Availability**

70

75

This work represents a synthesis of multiple independent research projects. The data needed to reproduce the tree-ring and coral data are publicly available through the NOAA National Centers for Environmental Information (Emile-Geay *et al.*, 2017; Walter *et al.*, 2023). The original Antarctic ice-core isotope data are archived at the PANGAEA database (Graf *et al.*, 2002) as well as the Greenland data except for core NGRIP whose data is available from the Centre for Ice and Climate of Copenhagen University (Weißbach *et al.*, 2016; Hörhold *et al.*, 2023). PANGAEA is hosted by the Alfred Wegener Institute Helmholtz Centre for Polar and Marine Research (AWI), Bremerhaven and the Center for Marine Environmental Sciences (MARUM), Bremen, Germany.

#### **Code Availability**

80

85

The general software to conduct the separation of signal and noise in the spectral domain and to perform the signal-to-noise ratio analysis is available as the R package proxysnr from the open research data repository Zenodo (Münch, 2018). Additionally, specific code to reproduce the tree-ring, coral, and ice-core analyses, respectively, are also available via Zenodo (McPartland 2024, Dolman 2024; Münch 2025 a,b).

#### **Author Contributions**

MYM wrote the manuscript, created figures, and contributed the analysis of tree-ring data. TM developed the signal-to-noise ratio analysis, contributed the analysis of the ice-core data, and helped write and edit the manuscript. AMD contributed analysis of coral data and the simulations of colored noise spectra and time uncertainty simulations, and helped write and edit the manuscript. RH helped write and edit the manuscript. TL developed the signal-to-noise ratio analysis, helped to write and edit the manuscript, and supervised analysis of all proxy data.

#### **Competing Interests**

The authors declare that they have no conflicts of interest.

### Acknowledgements

This is a contribution to the SPACE ERC project; this project has received funding from the European Research Council (ERC) under the European Union's Horizon 2020 research and innovation program (Grant Agreement 716092). A. Dolman was supported by the Deutsche Forschungsgemeinschaft (DFG, German Research Foundation) – Project number 468685498 (A.M.D.) – SPP 2299/Project number 441832482. T. Münch was supported by the Informationsinfrastrukturen Grant of the Helmholtz Association as part of the DataHub of the Research Field Earth and Environment. We acknowledge support by the Open Access Publication Funds of Alfred-Wegener-Institut Helmholtz-Zentrum für Polar- und Meeresforschung. The work profited from discussions at the Climate Variability Across Scales (CVAS) working group of the Past Global Changes (PAGES) program. We acknowledge the contributions of Nora Hirsch, Jannis Viola and Vanessa Skiba, along with members of the AWI-Earth System Diagnostics Group.

#### References

Ammann, C. M. and Wahl, E. R.: The importance of the geophysical context in statistical evaluations of climate reconstruction procedures, Climatic Change, 85, 71–88, <a href="https://doi.org/10.1007/s10584-007-9276-x">https://doi.org/10.1007/s10584-007-9276-x</a>, 2007.

- Ault, T. R., Cole, J. E., Overpeck, J. T., Pederson, G. T., St. George, S., Otto-Bliesner, B., Woodhouse, C. A., and Deser, C.: The Continuum of Hydroclimate Variability in Western North America during the Last Millennium, J. Climate, 26, 5863–5878, https://doi.org/10.1175/JCLI-D-11-00732.1, 2013.
- Berger, W. H., Johnson, R. F., and Killingley, J. S.: 'Unmixing' of the deep-sea record and the deglacial meltwater spike, Nature, 269, 661–663, https://doi.org/10.1038/269661a0, 1977.
  - Berkelmans, R. and van Oppen, M. J. H.: The role of zooxanthellae in the thermal tolerance of corals: a 'nugget of hope' for coral reefs in an era of climate change, Proceedings of the Royal Society B: Biological Sciences, 273, 2305–2312, https://doi.org/10.1098/rspb.2006.3567, 2006.
- Bothe, O., Wagner, S., and Zorita, E.: Simple noise estimates and pseudoproxies for the last 21 000 years, Earth System Science Data, 11, 1129–1152, <a href="https://doi.org/10.5194/essd-11-1129-2019">https://doi.org/10.5194/essd-11-1129-2019</a>, 2019.
  - Briffa, K. R. and Melvin, T. M.: A Closer Look at Regional Curve Standardization of Tree-Ring Records: Justification of the Need, a Warning of Some Pitfalls, and Suggested Improvements in Its
- 20 Application, in: Dendroclimatology, Springer, Dordrecht, 113–145, <a href="https://doi.org/10.1007/978-1-4020-5725-0">https://doi.org/10.1007/978-1-4020-5725-0</a> 5, 2011.
  - Casado, M., Münch, T., and Laepple, T.: Climatic information archived in ice cores: impact of intermittency and diffusion on the recorded isotopic signal in Antarctica, Climate of the Past, 16, 1581–1598, <a href="https://doi.org/10.5194/cp-16-1581-2020">https://doi.org/10.5194/cp-16-1581-2020</a>, 2020.
- Cheung, A. H., Mann, M. E., Steinman, B. A., Frankcombe, L. M., England, M. H., and Miller, S. K.: Comparison of Low-Frequency Internal Climate Variability in CMIP5 Models and Observations, J. Climate, 30, 4763–4776, https://doi.org/10.1175/JCLI-D-16-0712.1, 2017.
  - Cohen, A. L.: The Effect of Algal Symbionts on the Accuracy of Sr/Ca Paleotemperatures from Coral, Science, 296, 331–333, https://doi.org/10.1126/science.1069330, 2002.
- Comboul, M., Emile-Geay, J., Evans, M. N., Mirnateghi, N., Cobb, K. M., and Thompson, D. M.: A probabilistic model of chronological errors in layer-counted climate proxies: applications to annually banded coral archives, Climate of the Past, 10, 825–841, https://doi.org/10.5194/cp-10-825-2014, 2014.
  - Cook, E. R.: The decomposition of tree-ring series for environmental studies, Tree-ring bulletin (USA), 1987.
- Cook, E. R. and Kairiukstis, L. A.: Methods of Dendrochronology: Applications in the Environmental Sciences, Springer Science & Business Media, 403 pp., 1990.
  - Cook, E. R. and Peters, K.: Calculating unbiased tree-ring indices for the study of climatic and environmental change, The Holocene, 7, 361–370, <a href="https://doi.org/10.1177/095968369700700314">https://doi.org/10.1177/095968369700700314</a>, 1997.

- Cook, E. R., Briffa, K. R., Meko, D. M., Graybill, D. A., and Funkhouser, G.: The "segment length curse" in long tree-ring chronology development for palaeoclimatic studies, The Holocene, 5, 229–237, <a href="https://doi.org/10.1177/095968369500500211">https://doi.org/10.1177/095968369500500211</a>, 1995.
  - Dee, S., Emile-Geay, J., Evans, M. N., Allam, A., Steig, E. J., and Thompson, D. m.: PRYSM: An open-source framework for PRoxY System Modeling, with applications to oxygen-isotope systems, Journal of Advances in Modeling Earth Systems, 7, 1220–1247,
- 45 https://doi.org/10.1002/2015MS000447, 2015.
  - Dee, S. G., Steiger, N. J., Emile-Geay, J., and Hakim, G. J.: On the utility of proxy system models for estimating climate states over the common era, J. Adv. Model. Earth Syst., 8, 1164–1179, <a href="https://doi.org/10.1002/2016MS000677">https://doi.org/10.1002/2016MS000677</a>, 2016.
- Dee, S. G., Parsons, L. A., Loope, G. R., Overpeck, J. T., Ault, T. R., and Emile-Geay, J.: Improved spectral comparisons of paleoclimate models and observations via proxy system modeling: Implications for multi-decadal variability, Earth and Planetary Science Letters, 476, 34–46, <a href="https://doi.org/10.1016/j.epsl.2017.07.036">https://doi.org/10.1016/j.epsl.2017.07.036</a>, 2017.
  - Dee, S. G., Russell, J. M., Morrill, C., Chen, Z., and Neary, A.: PRYSM v2.0: A Proxy System Model for Lacustrine Archives, Paleoceanography and Paleoclimatology, 33, 1250–1269,
- 55 https://doi.org/10.1029/2018PA003413, 2018.
  - D'Olivo, J. P. and McCulloch, M. T.: Response of coral calcification and calcifying fluid composition to thermally induced bleaching stress, Sci Rep, 7, 2207, <a href="https://doi.org/10.1038/s41598-017-02306-x">https://doi.org/10.1038/s41598-017-02306-x</a>, 2017.
- D'Olivo, J. P., Georgiou, L., Falter, J., DeCarlo, T. M., Irigoien, X., Voolstra, C. R., Roder, C., Trotter, J., and McCulloch, M. T.: Long-Term Impacts of the 1997–1998 Bleaching Event on the Growth and Resilience of Massive Porites Corals From the Central Red Sea, Geochemistry, Geophysics, Geosystems, 20, 2936–2954, https://doi.org/10.1029/2019GC008312, 2019.
  - Dolman, A.: EarthSystemDiagnostics/Dolman-et-al-2024-corals-exaggerate: Code for second submission of paper, https://doi.org/10.5281/zenodo.14025394, 2024.
- Dolman, A., McPartland, M., Felis, T., and Laepple, T.: [preprint] Coral records exaggerate past decadal tropical climate variability, https://doi.org/10.21203/rs.3.rs-3924954/v1, 9 January 2025.
  - Dolman, A. M. and Laepple, T.: Sedproxy: a forward model for sediment-archived climate proxies, Climate of the Past, 14, 1851–1868, <a href="https://doi.org/10.5194/cp-14-1851-2018">https://doi.org/10.5194/cp-14-1851-2018</a>, 2018.
- Dolman, A. M., Kunz, T., Groeneveld, J., and Laepple, T.: A spectral approach to estimating the timescale-dependent uncertainty of paleoclimate records Part 2: Application and interpretation, Climate of the Past, 17, 825–841, <a href="https://doi.org/10.5194/cp-17-825-2021">https://doi.org/10.5194/cp-17-825-2021</a>, 2021a.

- Dolman, A. M., Groeneveld, J., Mollenhauer, G., Ho, S. L., and Laepple, T.: Estimating Bioturbation From Replicated Small-Sample Radiocarbon Ages, Paleoceanography and Paleoclimatology, 36, e2020PA004142, https://doi.org/10.1029/2020PA004142, 2021b.
- Emile-Geay, J., McKay, N. P., Kaufman, D. S., von Gunten, L., Wang, J., Anchukaitis, K. J., Abram, N. J., Addison, J. A., Curran, M. A. J., Evans, M. N., Henley, B. J., Hao, Z., Martrat, B., McGregor, H. V., Neukom, R., Pederson, G. T., Stenni, B., Thirumalai, K., Werner, J. P., Xu, C., Divine, D. V., Dixon, B., Gergis, J., Mundo, I. A., Nakatsuka, T., Phipps, S. J., Routson, C., Steig, E. J., Tierney, J. E., Tyler, J. J., Allen, K. J., Bertler, N. A. N., Björklund, J., Chase, B. M., Chen, M.-T., Cook, E. R., de Jong, R.,
- DeLong, K. L., Dixon, D. A., Ekaykin, A. A., Ersek, V., Filipsson, H. L., Francus, P., Freund, M. B., Frezzotti, M., Gaire, N. P., Gajewski, K. J., Ge, Q., Goosse, H., Gornostaeva, A., Grosjean, M., Horiuchi, K., Hormes, A., Husum, K., Isaksson, E., Kandasamy, K., Kawamura, K., Kilbourne, K. H., Koç, N., Leduc, G., Linderholm, H. W., Lorrey, A., Mikhalenko, V. N., Mortyn, P. G., Motoyama, H., Moy, A. D., Mulvaney, R., Munz, P. M., Nash, D. J., Oerter, H., Opel, T., Orsi, A. J., Ovchinnikov, D.
- V., Porter, T. J., Roop, H. A., Saenger, C. P., Sano, M., Sauchyn, D. J., Saunders, K. M., Seidenkrantz, M.-S., Severi, M., Shao, X., Sicre, M.-A., Sigl, M., Sinclair, K., St. George, S., St. Jacques, J.-M., Meloth, T., Thapa, U. K., Thomas, E. R., Turney, C. S. M., Uemura, R., Viau, A. E., Vladimirova, D. O., Wahl, E. R., White, J. W. C., Yu, Z., and Zinke, J.: NOAA/WDS Paleoclimatology PAGES2k Global 2,000 Year Multiproxy Database, https://doi.org/10.25921/YCR3-7588, 2017.
- EPICA community members: One-to-one coupling of glacial climate variability in Greenland and Antarctica, Nature, 444, 195–198, <a href="https://doi.org/10.1038/nature05301">https://doi.org/10.1038/nature05301</a>, 2006.
  - Esper, J. and Frank, D.: Divergence pitfalls in tree-ring research, Climatic Change, 94, 261–266, https://doi.org/10.1007/s10584-009-9594-2, 2009.
- Esper, J., Cook, E. R., Krusic, P. J., Peters, K., and Schweingruber, F. H.: Tests of the RCS Method for Preserving Low-Frequency Variability in Long Tree-Ring Chronologies, 2003.
  - Esper, J., Schneider, L., Smerdon, J. E., Schöne, B. R., and Büntgen, U.: Signals and memory in treering width and density data, Dendrochronologia, 35, 62–70, <a href="https://doi.org/10.1016/j.dendro.2015.07.001">https://doi.org/10.1016/j.dendro.2015.07.001</a>, 2015.
- Evans, M. N., Tolwinski-Ward, S. E., Thompson, D. M., and Anchukaitis, K. J.: Applications of proxy system modeling in high resolution paleoclimatology, Quaternary Science Reviews, 76, 16–28, <a href="https://doi.org/10.1016/j.quascirev.2013.05.024">https://doi.org/10.1016/j.quascirev.2013.05.024</a>, 2013.
  - Evans, M. N., Smerdon, J. E., Kaplan, A., Tolwinski-Ward, S. E., and González-Rouco, J. F.: Climate field reconstruction uncertainty arising from multivariate and nonlinear properties of predictors, Geophysical Research Letters, 41, 9127–9134, <a href="https://doi.org/10.1002/2014GL062063">https://doi.org/10.1002/2014GL062063</a>, 2014.
- Fisher, D. A., Reeh, N., and Clausen, H. B.: Stratigraphic Noise in Time Series Derived from Ice Cores, Annals of Glaciology, 7, 76–83, <a href="https://doi.org/10.3189/S0260305500005942">https://doi.org/10.3189/S0260305500005942</a>, 1985.

- Fraedrich, K. and Blender, R.: Scaling of Atmosphere and Ocean Temperature Correlations in Observations and Climate Models, Phys. Rev. Lett., 90, 108501, <a href="https://doi.org/10.1103/PhysRevLett.90.108501">https://doi.org/10.1103/PhysRevLett.90.108501</a>, 2003.
- Franke, J., Frank, D., Raible, C. C., Esper, J., and Brönnimann, S.: Spectral biases in tree-ring climate proxies, Nature Clim Change, 3, 360–364, <a href="https://doi.org/10.1038/nclimate1816">https://doi.org/10.1038/nclimate1816</a>, 2013.
  - Fritts, H.: Tree Rings and Climate, Elsevier, 583 pp., 1976.
- Gómez-Navarro, J. J., Zorita, E., Raible, C. C., and Neukom, R.: Pseudo-proxy tests of the analogue method to reconstruct spatially resolved global temperature during the Common Era, Climate of the Past, 13, 629–648, https://doi.org/10.5194/cp-13-629-2017, 2017.
  - Goodkin, N. F., Hughen, K. A., Cohen, A. L., and Smith, S. R.: Record of Little Ice Age sea surface temperatures at Bermuda using a growth-dependent calibration of coral Sr/Ca, Paleoceanography, 20, https://doi.org/10.1029/2005PA001140, 2005.
- Goosse, H., Crespin, E., de Montety, A., Mann, M. E., Renssen, H., and Timmermann, A.:
  Reconstructing surface temperature changes over the past 600 years using climate model simulations with data assimilation, Journal of Geophysical Research: Atmospheres, 115, <a href="https://doi.org/10.1029/2009JD012737">https://doi.org/10.1029/2009JD012737</a>, 2010.
  - Stable-isotope records from Dronning Maud Land, Antarctica:
- Haam, E. and Huybers, P.: A test for the presence of covariance between time-uncertain series of data with application to the Dongge Cave speleothem and atmospheric radiocarbon records, Paleoceanography, 25, 14 PP., <a href="https://doi.org/201010.1029/2008PA001713">https://doi.org/201010.1029/2008PA001713</a>, 2010.
  - Hasselmann, K.: Stochastic climate models Part I. Theory, Tellus, 28, 473–485, <a href="https://doi.org/10.3402/tellusa.v28i6.11316">https://doi.org/10.3402/tellusa.v28i6.11316</a>, 1976.
- Hayashi, E., Suzuki, A., Nakamura, T., Iwase, A., Ishimura, T., Iguchi, A., Sakai, K., Okai, T., Inoue, M., Araoka, D., Murayama, S., and Kawahata, H.: Growth-rate influences on coral climate proxies tested by a multiple colony culture experiment, Earth and Planetary Science Letters, 362, 198–206, https://doi.org/10.1016/j.epsl.2012.11.046, 2013.
  - Hébert, R., Rehfeld, K., and Laepple, T.: Comparing estimation techniques for timescale-dependent scaling of climate variability in paleoclimate time series, Nonlinear Processes in Geophysics
- 35 Discussions, 1–26, <a href="https://doi.org/10.5194/npg-2021-7">https://doi.org/10.5194/npg-2021-7</a>, 2021.
  - Hirsch, N., Zuhr, A., Münch, T., Hörhold, M., Freitag, J., Dallmayr, R., and Laepple, T.: Stratigraphic noise and its potential drivers across the plateau of Dronning Maud Land, East Antarctica, The Cryosphere, 17, 4207–4221, <a href="https://doi.org/10.5194/tc-17-4207-2023">https://doi.org/10.5194/tc-17-4207-2023</a>, 2023.

- Hollyman, P. R., Laptikhovsky, V. V., and Richardson, C. A.: Techniques for Estimating the Age and Growth of Molluscs: Gastropoda, shre, 37, 773–782, <a href="https://doi.org/10.2983/035.037.0408">https://doi.org/10.2983/035.037.0408</a>, 2018.
  - Hörhold, M., Münch, T., Weißbach, S., Kipfstuhl, S., Freitag, J., Sasgen, I., Lohmann, G., Vinther, B., and Laepple, T.: Modern temperatures in central—north Greenland warmest in past millennium, Nature, 613, 503–507, <a href="https://doi.org/10.1038/s41586-022-05517-z">https://doi.org/10.1038/s41586-022-05517-z</a>, 2023.
- Hughes, M. K. and Ammann, C. M.: The future of the past—an earth system framework for high resolution paleoclimatology: editorial essay, Climatic Change, 94, 247–259, https://doi.org/10.1007/s10584-009-9588-0, 2009.
  - Hutson, W. H.: Bioturbation of deep-sea sediments: Oxygen isotopes and stratigraphic uncertainty, Geology, 8, 127–130, <a href="https://doi.org/10.1130/0091-7613(1980)8%253C127:BODSOI%253E2.0.CO;2">https://doi.org/10.1130/0091-7613(1980)8%253C127:BODSOI%253E2.0.CO;2</a>, 1980.
- Huybers, P. and Curry, W.: Links between annual, Milankovitch and continuum temperature variability, Nature, 441, 329–332, https://doi.org/10.1038/nature04745, 2006.
  - Johnsen, S. J., Clausen, H. B., Cuffey, K. M., Hoffmann, G., Schwander, J., and Creyts, T.: Diffusion of stable isotopes in polar firn and ice: the isotope effect in firn diffusion, in: Physics of Ice Core Records, vol. 159, edited by: Hondoh, T., Hokkaido University Press, Sapporo, Japan, 121–140, 2000.
- Jones, D. S.: Sclerochronology: Reading the Record of the Molluscan Shell: Annual growth increments in the shells of bivalve molluscs record marine climatic changes and reveal surprising longevity, American Scientist, 71, 384–391, 1983.
  - Jones, P. D., Briffa, K. R., Osborn, T. J., Lough, J. M., van Ommen, T. D., Vinther, B. M., Luterbacher, J., Wahl, E. R., Zwiers, F. W., Mann, M. E., Schmidt, G. A., Ammann, C. M., Buckley, B. M., Cobb, K.
- M., Esper, J., Goosse, H., Graham, N., Jansen, E., Kiefer, T., Kull, C., Küttel, M., Mosley-Thompson, E., Overpeck, J. T., Riedwyl, N., Schulz, M., Tudhope, A. W., Villalba, R., Wanner, H., Wolff, E., and Xoplaki, E.: High-resolution palaeoclimatology of the last millennium: a review of current status and future prospects, The Holocene, 19, 3–49, <a href="https://doi.org/10.1177/0959683608098952">https://doi.org/10.1177/0959683608098952</a>, 2009.
- King, J. M., Anchukaitis, K. J., Tierney, J. E., Hakim, G. J., Emile-Geay, J., Zhu, F., and Wilson, R.: A
  Data Assimilation Approach to Last Millennium Temperature Field Reconstruction Using a Limited
  High-Sensitivity Proxy Network, <a href="https://doi.org/10.1175/JCLI-D-20-0661.1">https://doi.org/10.1175/JCLI-D-20-0661.1</a>, 2021.
  - Kunz, T., Dolman, A. M., and Laepple, T.: A spectral approach to estimating the timescale-dependent uncertainty of paleoclimate records Part 1: Theoretical concept, Climate of the Past, 16, 1469–1492, <a href="https://doi.org/10.5194/cp-16-1469-2020">https://doi.org/10.5194/cp-16-1469-2020</a>, 2020.

- Laepple, T. and Huybers, P.: Reconciling discrepancies between Uk37 and Mg/Ca reconstructions of Holocene marine temperature variability, Earth and Planetary Science Letters, 375, 418–429, <a href="https://doi.org/10.1016/j.epsl.2013.06.006">https://doi.org/10.1016/j.epsl.2013.06.006</a>, 2013.
  - Laepple, T., Münch, T., Casado, M., Hoerhold, M., Landais, A., and Kipfstuhl, S.: On the similarity and apparent cycles of isotopic variations in East Antarctic snow pits, The Cryosphere, 12, 169–187, https://doi.org/10.5194/tc-12-169-2018, 2018.
  - Lee, T. C. K., Zwiers, F. W., and Tsao, M.: Evaluation of proxy-based millennial reconstruction methods, Clim Dyn, 31, 263–281, https://doi.org/10.1007/s00382-007-0351-9, 2008.

85

- Little, A. F., van Oppen, M. J. H., and Willis, B. L.: Flexibility in Algal Endosymbioses Shapes Growth in Reef Corals, Science, 304, 1492–1494, <a href="https://doi.org/10.1126/science.1095733">https://doi.org/10.1126/science.1095733</a>, 2004.
- Lough, J. M.: A strategy to improve the contribution of coral data to high-resolution paleoclimatology, Palaeogeography, Palaeoclimatology, Palaeoecology, 204, 115–143, <a href="https://doi.org/10.1016/S0031-0182(03)00727-2">https://doi.org/10.1016/S0031-0182(03)00727-2</a>, 2004.
  - Lücke, L. J., Hegerl, G. C., Schurer, A. P., and Wilson, R.: Effects of Memory Biases on Variability of Temperature Reconstructions, Journal of Climate, 32, 8713–8731, <a href="https://doi.org/10.1175/JCLI-D-19-0184.1">https://doi.org/10.1175/JCLI-D-19-0184.1</a>, 2019.
    - Maier, C., Felis, T., Pätzold, J., and Bak, R. P. M.: Effect of skeletal growth and lack of species effects in the skeletal oxygen isotope climate signal within the coral genus Porites, Marine Geology, 207, 193–208, <a href="https://doi.org/10.1016/j.margeo.2004.03.008">https://doi.org/10.1016/j.margeo.2004.03.008</a>, 2004.
- Mann, M. E. and Rutherford, S.: Climate reconstruction using 'Pseudoproxies,' Geophysical Research Letters, 29, 139-1-139–4, https://doi.org/10.1029/2001GL014554, 2002.
  - Mann, M. E., Rutherford, S., Wahl, E., and Ammann, C.: Testing the Fidelity of Methods Used in Proxy-Based Reconstructions of Past Climate, Journal of Climate, 18, 4097–4107, <a href="https://doi.org/10.1175/JCLI3564.1">https://doi.org/10.1175/JCLI3564.1</a>, 2005.
- Mann, M. E., Rutherford, S., Wahl, E., and Ammann, C.: Robustness of proxy-based climate field reconstruction methods, Journal of Geophysical Research: Atmospheres, 112, <a href="https://doi.org/10.1029/2006JD008272">https://doi.org/10.1029/2006JD008272</a>, 2007.
  - Matalas, N. C.: Statistical Properties of Tree Ring Data, International Association of Scientific Hydrology. Bulletin, 7, 39–47, <a href="https://doi.org/10.1080/02626666209493254">https://doi.org/10.1080/02626666209493254</a>, 1962.
- McCulloch, M. T., Winter, A., Sherman, C. E., and Trotter, J. A.: 300 years of sclerosponge thermometry shows global warming has exceeded 1.5 °C, Nat. Clim. Chang., 14, 171–177, <a href="https://doi.org/10.1038/s41558-023-01919-7">https://doi.org/10.1038/s41558-023-01919-7</a>, 2024.

- McPartland, M. Y.: EarthSystemDiagnostics/McPartland\_etal\_2024\_DendroSNR: v1.1, https://doi.org/10.5281/zenodo.10822165, 2024.
- McPartland, M. Y., St. George, S., Pederson, G. T., and Anchukaitis, K. J.: Does signal-free detrending increase chronology coherence in large tree-ring networks?, Dendrochronologia, 125755, <a href="https://doi.org/10.1016/j.dendro.2020.125755">https://doi.org/10.1016/j.dendro.2020.125755</a>, 2020.
  - McPartland, M. Y., Dolman, A. M., and Laepple, T.: Separating Common Signal From Proxy Noise in Tree Rings, Geophysical Research Letters, 51, e2024GL109282, https://doi.org/10.1029/2024GL109282, 2024.
- 10 Meko, D. M.: Applications of Box-Jenkins methods of time series analysis to the reconstruction of drought from tree rings, 1981.
  - Melvin, T. M. and Briffa, K. R.: A "signal-free" approach to dendroclimatic standardisation, Dendrochronologia, 26, 71–86, <a href="https://doi.org/10.1016/j.dendro.2007.12.001">https://doi.org/10.1016/j.dendro.2007.12.001</a>, 2008.
- Melvin, T. M. and Briffa, K. R.: CRUST: Software for the implementation of Regional Chronology Standardisation: Part 1. Signal-Free RCS, Dendrochronologia, 32, 7–20, https://doi.org/10.1016/j.dendro.2013.06.002, 2014a.
  - Melvin, T. M. and Briffa, K. R.: CRUST: Software for the implementation of Regional Chronology Standardisation: Part 2. Further RCS options and recommendations, Dendrochronologia, 32, 343–356, <a href="https://doi.org/10.1016/j.dendro.2014.07.008">https://doi.org/10.1016/j.dendro.2014.07.008</a>, 2014b.
- Münch, T. proxysnr: An R package to separate the common signal from local noise in climate proxy records using spectral analyses (v1.0.1). Zenodo.https://doi.org/10.5281/zenodo.17098991, 2025.
  - Münch, T. ice-colors-of-noise: R software to perform signal-to-noise ratio analyses for Greenland and Antarctic ice-core data (v0.1.0). Zenodo. <a href="https://doi.org/10.5281/zenodo.17102273">https://doi.org/10.5281/zenodo.17102273</a>, (2025).
- Münch, T. and Laepple, T.: What climate signal is contained in decadal- to centennial-scale isotope variations from Antarctic ice cores?, Climate of the Past, 14, 2053–2070, <a href="https://doi.org/10.5194/cp-14-2053-2018">https://doi.org/10.5194/cp-14-2053-2018</a>, 2018.
  - Münch, T., Werner, M., and Laepple, T.: How precipitation intermittency sets an optimal sampling distance for temperature reconstructions from Antarctic ice cores, Climate of the Past, 17, 1587–1605, <a href="https://doi.org/10.5194/cp-17-1587-2021">https://doi.org/10.5194/cp-17-1587-2021</a>, 2021.
- Neukom, R., Steiger, N., Gómez-Navarro, J. J., Wang, J., and Werner, J. P.: No evidence for globally coherent warm and cold periods over the preindustrial Common Era, Nature, 571, 550–554, <a href="https://doi.org/10.1038/s41586-019-1401-2">https://doi.org/10.1038/s41586-019-1401-2</a>, 2019.

- PAGES2k Consortium, Emile-Geay, J., McKay, N. P., Kaufman, D. S., Gunten, L. von, Wang, J., Anchukaitis, K. J., Abram, N. J., Addison, J. A., Curran, M. A. J., Evans, M. N., Henley, B. J., Hao, Z.,
- Martrat, B., McGregor, H. V., Neukom, R., Pederson, G. T., Stenni, B., Thirumalai, K., Werner, J. P., Xu, C., Divine, D. V., Dixon, B. C., Gergis, J., Mundo, I. A., Nakatsuka, T., Phipps, S. J., Routson, C. C., Steig, E. J., Tierney, J. E., Tyler, J. J., Allen, K. J., Bertler, N. A. N., Björklund, J., Chase, B. M., Chen, M.-T., Cook, E., Jong, R. de, DeLong, K. L., Dixon, D. A., Ekaykin, A. A., Ersek, V., Filipsson, H. L., Francus, P., Freund, M. B., Frezzotti, M., Gaire, N. P., Gajewski, K., Ge, Q., Goosse, H.,
- Gornostaeva, A., Grosjean, M., Horiuchi, K., Hormes, A., Husum, K., Isaksson, E., Kandasamy, S., Kawamura, K., Kilbourne, K. H., Koç, N., Leduc, G., Linderholm, H. W., Lorrey, A. M., Mikhalenko, V., Mortyn, P. G., Motoyama, H., Moy, A. D., Mulvaney, R., Munz, P. M., Nash, D. J., Oerter, H., Opel, T., Orsi, A. J., Ovchinnikov, D. V., Porter, T. J., Roop, H. A., Saenger, C., Sano, M., Sauchyn, D., Saunders, K. M., Seidenkrantz, M.-S., Severi, M., Shao, X., Sicre, M.-A., Sigl, M., Sinclair, K., George,
- S. S., Jacques, J.-M. S., Thamban, M., Thapa, U. K., Thomas, E. R., Turney, C., Uemura, R., Viau, A. E., Vladimirova, D. O., Wahl, E. R., White, J. W. C., Yu, Z., and Zinke, J.: A global multiproxy database for temperature reconstructions of the Common Era, Scientific Data, 4, 170088, <a href="https://doi.org/10.1038/sdata.2017.88">https://doi.org/10.1038/sdata.2017.88</a>, 2017.
- Pelletier, J. D.: The power spectral density of atmospheric temperature from time scales of 10–2 to 106 yr, Earth and Planetary Science Letters, 158, 157–164, <a href="https://doi.org/10.1016/S0012-821X(98)00051-X">https://doi.org/10.1016/S0012-821X(98)00051-X</a>, 1998.
  - Peng, T.-H. and Broecker, W. S.: The impacts of bioturbation on the age difference between benthic and planktonic foraminifera in deep sea sediments, Nuclear Instruments and Methods in Physics Research Section B: Beam Interactions with Materials and Atoms, 5, 346–352,
- 55 https://doi.org/10.1016/0168-583X(84)90540-8, 1984.

- Percival, D. B. and Walden, A. T.: Spectral Analysis for Physical Applications, Cambridge University Press, 616 pp., 1993.
- Reschke, M., Rehfeld, K., and Laepple, T.: Empirical estimate of the signal content of Holocene temperature proxy records, Climate of the Past, 15, 521–537, <a href="https://doi.org/10.5194/cp-15-521-2019">https://doi.org/10.5194/cp-15-521-2019</a>, 2019.
- Rhines, A. and Huybers, P.: Estimation of spectral power laws in time uncertain series of data with application to the Greenland Ice Sheet Project 2  $\delta^{18}$ O record, Journal of Geophysical Research: Atmospheres, 116, <a href="https://doi.org/10.1029/2010JD014764">https://doi.org/10.1029/2010JD014764</a>, 2011.
- Riedwyl, N., Küttel, M., Luterbacher, J., and Wanner, H.: Comparison of climate field reconstruction techniques: application to Europe, Clim Dyn, 32, 381–395, <a href="https://doi.org/10.1007/s00382-008-0395-5">https://doi.org/10.1007/s00382-008-0395-5</a>, 2009.

- Ruddiman, W. F., Jones, G. A., Peng, T.-H., Glover, L. K., Glass, B. P., and Liebertz, P. J.: Tests for size and shape dependency in deep-sea mixing, Sedimentary Geology, 25, 257–276, <a href="https://doi.org/10.1016/0037-0738(80)90064-0">https://doi.org/10.1016/0037-0738(80)90064-0</a>, 1980.
- Rypel, A. L., Haag, W. R., and Findlay, R. H.: Validation of annual growth rings in freshwater mussel shells using cross dating, Can. J. Fish. Aquat. Sci., 65, 2224–2232, <a href="https://doi.org/10.1139/F08-129">https://doi.org/10.1139/F08-129</a>, 2008.
  - Saenger, C., Cohen, A. L., Oppo, D. W., and Hubbard, D.: Interpreting sea surface temperature from strontium/calcium ratios in Montastrea corals: Link with growth rate and implications for proxy reconstructions, Paleoceanography, 23, https://doi.org/10.1029/2007PA001572, 2008.
  - Schiffelbein, P.: Calculation of error measures for deconvolved deep-sea stratigraphic records, Marine Geology, 65, 333–342, https://doi.org/10.1016/0025-3227(85)90063-5, 1985.
  - Schiffelbein, P. and Hills, S.: Direct assessment of stable isotope variability in planktonic foraminifera populations, Palaeogeography, Palaeoclimatology, Palaeoecology, 48, 197–213,
- 80 https://doi.org/10.1016/0031-0182(84)90044-0, 1984.

- Scott, R. B., Holland, C. L., and Quinn, T. M.: Multidecadal Trends in Instrumental SST and Coral Proxy Sr/Ca Records, Journal of Climate, 23, 1017–1033, <a href="https://doi.org/10.1175/2009JCLI2386.1">https://doi.org/10.1175/2009JCLI2386.1</a>, 2010.
- Shaw, F., Dolman, A. M., Kunz, T., Gkinis, V., and Laepple, T.: Novel approach to estimate the water isotope diffusion length in deep ice cores with an application to MIS 19 in the EPICA Dome C ice core, EGUsphere, 1–18, <a href="https://doi.org/10.5194/egusphere-2023-2549">https://doi.org/10.5194/egusphere-2023-2549</a>, 2023.
  - Shaw, F., Dolman, A. M., Kunz, T., Gkinis, V., and Laepple, T.: Novel approach to estimate the water isotope diffusion length in deep ice cores with an application to Marine Isotope Stage 19 in the Dome C ice core, The Cryosphere, 18, 3685–3698, <a href="https://doi.org/10.5194/tc-18-3685-2024">https://doi.org/10.5194/tc-18-3685-2024</a>, 2024.
- Smerdon, J. E.: Climate models as a test bed for climate reconstruction methods: pseudoproxy experiments, WIREs Climate Change, 3, 63–77, <a href="https://doi.org/10.1002/wcc.149">https://doi.org/10.1002/wcc.149</a>, 2012.
  - Smerdon, J. E., Kaplan, A., Chang, D., and Evans, M. N.: A Pseudoproxy Evaluation of the CCA and RegEM Methods for Reconstructing Climate Fields of the Last Millennium, <a href="https://doi.org/10.1175/2010JCLI3328.1">https://doi.org/10.1175/2010JCLI3328.1</a>, 2010.
- 95 Speer, J. H.: Fundamentals of Tree-ring Research, University of Arizona Press, 370 pp., 2010.
  - Stenni, B., Curran, M. A. J., Abram, N. J., Orsi, A., Goursaud, S., Masson-Delmotte, V., Neukom, R., Goosse, H., Divine, D., van Ommen, T., Steig, E. J., Dixon, D. A., Thomas, E. R., Bertler, N. A. N., Isaksson, E., Ekaykin, A., Werner, M., and Frezzotti, M.: Antarctic climate variability on regional and

- continental scales over the last 2000 years, Clim. Past, 13, 1609–1634, <a href="https://doi.org/10.5194/cp-13-1609-2017">https://doi.org/10.5194/cp-13-1609-2017</a>, 2017.
  - von Storch, H., Zorita, E., Jones, J. M., Dimitriev, Y., González-Rouco, F., and Tett, S. F. B.: Reconstructing Past Climate from Noisy Data, Science, 306, 679–682, https://doi.org/10.1126/science.1096109, 2004.
- von Storch, H., Zorita, E., and González-Rouco, F.: Assessment of three temperature reconstruction methods in the virtual reality of a climate simulation, Int J Earth Sci (Geol Rundsch), 98, 67–82, https://doi.org/10.1007/s00531-008-0349-5, 2009.
  - Suzuki, A., Hibino, K., Iwase, A., and Kawahata, H.: Intercolony variability of skeletal oxygen and carbon isotope signatures of cultured Porites corals: Temperature-controlled experiments, Geochimica et Cosmochimica Acta, 69, 4453–4462, https://doi.org/10.1016/j.gca.2005.05.018, 2005.
- Tolwinski-Ward, S. E., Evans, M. N., Hughes, M. K., and Anchukaitis, K. J.: An efficient forward model of the climate controls on interannual variation in tree-ring width, Clim Dyn, 36, 2419–2439, https://doi.org/10.1007/s00382-010-0945-5, 2011.
- Vaganov, E. A., Anchukaitis, K. J., and Evans, M. N.: How Well Understood Are the Processes that Create Dendroclimatic Records? A Mechanistic Model of the Climatic Control on Conifer Tree-Ring Growth Dynamics, in: Dendroclimatology: Progress and Prospects, edited by: Hughes, M. K., Swetnam, T. W., and Diaz, H. F., Springer Netherlands, Dordrecht, 37–75, <a href="https://doi.org/10.1007/978-1-4020-5725-0">https://doi.org/10.1007/978-1-4020-5725-0</a> 3, 2011.
- Vautard, R. and Ghil, M.: Singular spectrum analysis in nonlinear dynamics, with applications to paleoclimatic time series, Physica D: Nonlinear Phenomena, 35, 395–424, <a href="https://doi.org/10.1016/0167-2789(89)90077-8">https://doi.org/10.1016/0167-2789(89)90077-8</a>, 1989.
  - Walter, R. M., Sayani, H. R., Felis, T., Cobb, K. M., Abram, N. J., Arzey, A. K., Atwood, A. R., Brenner, L. D., Dassié, É. P., DeLong, K. L., Ellis, B., Emile-Geay, J., Fischer, M. J., Goodkin, N. F., Hargreaves, J. A., Kilbourne, K. H., Krawczyk, H., McKay, N. P., Moore, A. L., Murty, S. A., Ong, M. R., Ramos, R. D., Reed, E. V., Samanta, D., Sanchez, S. C., Zinke, J., and the PAGES CoralHydro2k
- Project Members: The CoralHydro2k database: a global, actively curated compilation of coral  $\delta$  <sup>18</sup> O and Sr/Ca proxy records of tropical ocean hydrology and temperature for the Common Era, Earth Syst. Sci. Data, 15, 2081–2116, https://doi.org/10.5194/essd-15-2081-2023, 2023.
  - Weißbach, S., Wegner, A., Opel, T., Oerter, H., Vinther, B. M., and Kipfstuhl, S.: Spatial and temporal oxygen isotope variability in northern Greenland implications for a new climate record over the past millennium, Climate of the Past, 12, 171–188, <a href="https://doi.org/10.5194/cp-12-171-2016">https://doi.org/10.5194/cp-12-171-2016</a>, 2016.

Whillans, I. M. and Grootes, P. M.: Isotopic diffusion in cold snow and firn, Journal of Geophysical Research: Atmospheres, 90, 3910–3918, <a href="https://doi.org/10.1029/JD090iD02p03910">https://doi.org/10.1029/JD090iD02p03910</a>, 1985.

- Zhang, H., Yuan, N., Esper, J., Werner, J. P., Xoplaki, E., Büntgen, U., Treydte, K., and Luterbacher, J.: Modified climate with long term memory in tree ring proxies, Environ. Res. Lett., 10, 084020,
- 35 https://doi.org/10.1088/1748-9326/10/8/084020, 2015.
  - Zhu, F., Emile-Geay, J., McKay, N. P., Hakim, G. J., Khider, D., Ault, T. R., Steig, E. J., Dee, S., and Kirchner, J. W.: Climate models can correctly simulate the continuum of global-average temperature variability, Proceedings of the National Academy of Sciences, 116, 8728–8733, <a href="https://doi.org/10.1073/pnas.1809959116">https://doi.org/10.1073/pnas.1809959116</a>, 2019.
- Zhu, F., Emile-Geay, J., McKay, N. P., Stevenson, S., and Meng, Z.: A pseudoproxy emulation of the PAGES 2k database using a hierarchy of proxy system models, Sci Data, 10, 624, https://doi.org/10.1038/s41597-023-02489-1, 2023.
  - Zuhr, A. M., Wahl, S., Steen-Larsen, H. C., Hörhold, M., Meyer, H., and Laepple, T.: A Snapshot on the Buildup of the Stable Water Isotopic Signal in the Upper Snowpack at EastGRIP on the Greenland
- Ice Sheet, Journal of Geophysical Research: Earth Surface, 128, e2022JF006767, https://doi.org/10.1029/2022JF006767, 2023.